Published in final edited form as:
IEEE Trans Neural Syst Rehabil Eng. 2010 February ; 18(1): 67–74. doi:10.1109/TNSRE.2009.2036849.

Bidirectional Telemetry Controller for Neuroprosthetic Devices

Vishnu Sharma, **Douglas B. McCreery**, **Martin Han [Member, IEEE]**, and **Victor Pikov**
Neural Engineering Program, Huntington Medical Research Institutes, Pasadena, CA 91105 USA

Vishnu Sharma: vishnu_vds@yahoo. com; Douglas B. McCreery: dougmc@hmri.org; Martin Han: martinhan@hmri.org; Victor Pikov: pikov@hotmail.com

Abstract

We present versatile multifunctional programmable controller with bidirectional data telemetry, implemented using existing commercial microchips and standard Bluetooth protocol, which adds convenience, reliability, and ease-of-use to neuroprosthetic devices. Controller, weighing 190 g, is placed on animal's back and provides bidirectional sustained telemetry rate of 500 kb/s, allowing real-time control of stimulation parameters and viewing of acquired data. In continuously-active state, controller consumes ~420 mW and operates without recharge for 8 h. It features independent 16-channel current-controlled stimulation, allowing current steering; customizable stimulus current waveforms; recording of stimulus voltage waveforms and evoked neuronal responses with stimulus artifact blanking circuitry. Flexibility, scalability, cost-efficiency, and a user-friendly computer interface of this device allow use in animal testing for variety of neuroprosthetic applications. Initial testing of the controller has been done in a feline model of brainstem auditory prosthesis. In this model, the electrical stimulation is applied to the array of microelectrodes implanted in the ventral cochlear nucleus, while the evoked neuronal activity was recorded with the electrode implanted in the contralateral inferior colliculus. Stimulus voltage waveforms to monitor the access impedance of the electrodes were acquired at the rate of 312 kilosamples/s. Evoked neuronal activity in the inferior colliculus was recorded after the blanking (transient silencing) of the recording amplifier during the stimulus pulse, allowing the detection of neuronal responses within 100 μs after the end of the stimulus pulse applied in the cochlear nucleus.

Index Terms

Bidirectional; electrode; neural prostheses; recording; stimulation; telemetry; wireless

I. Introduction

PRESENT and anticipated uses of neuroprosthetic and neuromodulation devices for rehabilitation and treatment of neurological disorders include deafness, blindness, Parkinson's disease, depression, epilepsy, spinal cord injury, amyotrophic lateral sclerosis, and stroke [1]–[9]. An increasing number of these devices require bidirectional data transfer to allow monitoring and adjustment of the stimulus parameters as well as monitoring of neuronal activity via the downlink.

For the development of novel neuroprosthetic devices, wireless communication offers several benefits, including continuous data recording without restricting the animal's mobility and avoiding the stress to the animals caused by constraint and tethering. Early biotelemetry controllers utilized unidirectional analog UHF for data uplink or downlink [10]–[12]. The devices with bidirectional telemetry employed specialized ASICs, making these devices costly

to develop and modify [13]–[15]. Recent development of compact high-power density Li-ion batteries allows extended battery life even at relatively high power consumption [16] and the availability of off-the-shelf components for digital wireless telecommunications protocols, such as Bluetooth and Wi-Fi/IEEE 802.11 [17], [18] allow increased data throughput, data security, automatic error detection and correction not present in analog communication protocols [19]. Bluetooth 2.0 class 2 protocol is particularly well-suited for short-range (< 10 m) and low-power (<2.5 mW) devices.[1]

In this article, we describe a prototype controller with bidirectional telemetry, utilizing commercial-grade off-the-shelf integrated-circuit (COTS IC) components, standard Bluetooth protocol, and a user-friendly graphical computer interface. This controller provides novel capabilities, including independent control of the stimulating channels, customizable controlled-stimulus current waveforms, and flexible control of stimulus timing, allowing any combination of simultaneous and interleaved pulsing across the array of 16 electrodes. The controller is sufficiently compact and lightweight to be worn by larger animals (e.g., cats and rabbits). By utilizing COTS IC components and standard Bluetooth protocols, the development has been cost-efficient and allows for future scalability and flexibility during the preclinical development of a variety of neuroprosthetic and neuromodulation devices.

II. Methods

A. System Description of the Controller

The principal modules of the wearable controller are the stimulation pattern generator (SPG) module, a module for recording the stimulus voltage waveforms (SVW) from the electrodes, and a module for recording the evoked neuronal responses (ENR) [Fig. 1(a)]. The SPG consists of 1) the stimulus pulse waveform generator, the trigger for synchronization with the SVW recording module, and the stimulus artifact-blanking pulse for synchronization with the ENR recording module; and 2) the electrode pattern generator which specifies the temporal pattern of the stimulation across the 16 stimulating electrodes. The digital stimulus pulse output of the pulse waveform generator is converted to a biphasic analog voltage which is directed through the switching bank to the bank of voltage-to-current converters (Howland current pumps). The switches are turned on and off either simultaneously or sequentially to produce the specified pattern of stimulation. The output of each voltage-to-current converters ranges from 1 to 100 μA.

The voltage-to-current converters include features to prevent injury to the neural tissue adjacent to the stimulating electrode in the event of a component failure, including partial or complete failure of the power supply. Each of the Howland pumps is coupled to its electrode through a 0.3 μF capacitor which prevents injection of a net charge. The capacitor value was selected to be large enough to avoid significant microelectrode polarization (less than 0.5 V), when applying the first phase of a biphasic pulse having relatively large charge (e.g., 150 nC/phase). Minimal microelectrode polarization is needed for preserving the voltage compliance of the Howland current pumps. The value of 0.3 μF satisfies this requirement.

On each channel, the electrode side of the capacitor is coupled through a 4 MΩ bias resistor (R_b) to an adjustable anodic bias voltage. The bias increases the charge injection capacity of the activated iridium electrode sites [20], [21]. The R_b value was selected to be much larger than the impedance of the microelectrodes at the range of frequencies comprising the spectrum of the electrode voltage transients (mostly above 1 kHz) in order not to divert a significant proportion of stimulus current from the Howland pump. The R_b value also must be much

[1] http://www.bluetooth.org

smaller than the dc impedance of the microelectrodes, so that differences in their dc impedance do not introduce significant variation in their anodic biases (all of the bias channels are driven from a single source). The bias voltage is derived from the main power bus via of a simple voltage divider circuit which limits the anodic bias voltage to an absolute maximum of 400 mV with respect to the platinum counter electrode, and thus below the potential for oxidative hydrolysis of water. We have used this design for many years [22]–[32] and have validated its safety for neural stimulation in different applications. In addition, there is a general power-line fuse to prevent overheating of the battery in the event of a circuit fault.

The SVWs induced by the stimulus pulses are monitored through a bank of 16 unity-gain buffers. The ENRs are considerably smaller (up to ±500 μV) as compared to the SVWs (up to ±8 V including the access voltage of the tissue), and the amplification in the ENR module is set at 1000× as opposed to 0.3 × in the SVW recording module. Level shifters in both recording modules are needed to convert the bipolar signals into positive-only signals, which are then digitized using A/D converters. SVW data is digitized at 8 bit and 312 kilosamples/s in order to capture rapid voltage dynamics at the beginning of the pulse, which is used for evaluating the access impedance of the electrodes. Recording of the SVWs begins 10 μs prior to the initiation of the stimulus pulse and proceeds for 630 μs until 196 samples are collected. The ENR data is digitized at 12 bit and 27 kilosamples/s. The beginning of the ENR recording is triggered by the trailing edge of the artifact-blanking pulse, generated by SPG 15 μs after the stimulus pulse termination, and proceeds until it is terminated by the leading edge of the next artifact-blanking pulse. The blanking (transient silencing) of high-gain (1000×) ENR amplifier during the stimulus pulse suppresses the stimulus artifact and allows the ENR amplifier to remain unsaturated and to commence its activity at 15 μs after the stimulus pulse [Fig. 1(b)].

Bidirectional telemetry allows user control of the SPG, continuous monitoring of the ENR and sequential transmission of SVW data from the stimulating electrodes. The Bluetooth microchip supports the standard Bluetooth protocol Version 2.0 + EDR, capable of 3 Mb/s data transmission rate. In the prototype device, we use a rate to 0.5 Mb/s, which is adequate for continuous transmission of 16-bit ENR data (4 bits not used) and periodic transmission of 8-bit SVW data at a stimulation rate to up to 100 Hz (stimulation interval ≥10 ms). Data transmission limitations of the Bluetooth protocol necessitate a sequential rather than simultaneous recording of the SVW. Therefore, the amplifier in the SVW recording module is preceded by a 16:1 multiplexer for electrode selection.

The above functions of the wearable controller have been implemented using the commercial microchip components listed in the Table I. The circuit diagram of the animal-worn controller is presented in Supplemental Figure 1 and the key physical and electrical parameters of the controller are summarized in Supplemental Table 1.

The wearable controller was fabricated on three interconnected printed circuit boards and is housed in a plastic enclosure measuring 13 × 6 × 3 cm (Fig. 2). The modular design will expedite development of future versions of controller with a higher number of stimulating and recorded channels. The packaged controller with two 1400 mAh batteries and attached animal cable weighs 190 g. Battery recharging and programming of the PIC microcontroller chips is done via three mini-USB connectors.

The wearable controller is powered by an 8.4 V lithium-polymer iPhone battery rated at 1400 mAh. The controller consumes ~418 mW with both microcontroller chips active, the Bluetooth chip in Rx&Tx mode, and during continuous stimulation of one of the electrodes. When the controller is operating autonomously between the hourly SVW checks, its power consumption is reduced to ~236 mW due to reduced power consumption of the Bluetooth chip and the Tx microcontroller in the standby mode. During the actual controller test with continuous ENR

transmission via the Tx microcontroller, the battery lasted for 8 h, while with the Tx microcontroller in standby mode for 59 min out of each hour, the battery life was extended to almost 11 h (Fig. 3).

B. Computer-Based Controller

The computer-based controller is composed of the USB Bluetooth transceiver and the software providing the graphical interface for the control of the SPG and for viewing and saving of the ENRs and SVWs (Fig. 4, Supplemental Figure 2). The user has flexible control of the stimulus waveform and of the temporal pattern of the stimulation across the simulating electrode array parameters, as well as the ability to initiate and terminate the stimulation and/or recording at will or at specified time intervals. The SVW data from all or a selected subset of the electrodes can be displayed. The software has been developed using Visual Basic 6 (Microsoft) with its built-in functions for data streaming to the hard drive and with several ActiveX controls, including: the Measurement Studio 8 (National Instruments) for graphical user interface, the LongTimer ActiveX (home.comcast.net) for timing recording and stimulating events over a wide range of intervals (from 1 ms to 24 days), and the MSComm ActiveX (Microsoft) for communication with the USB Bluetooth transceiver via a virtual serial port.

Display and saving of the recorded data requires frequent asynchronous interaction with the wearable controller, which is accomplished by embedding 16-bit flags inside a continuous data stream. In Fig. 5, two typical data acquisition tasks are shown: the first is the user-initiated saving of the ENRs during a sequence of stimulation amplitudes and the second is automated periodic saving of the SVWs for measurement of electrode impedance. Since changes in electrode impedance typically occurs over a course of many hours of stimulation, the SVWs are saved once per hour using a software timer, while the data between the saves is displayed on the monitor and then discarded.

III. Results

The wearable controller was evaluated with an array of 16 microstimulation sites [33], implanted in the ventral cochlear nucleus and with a bipolar electrode for simultaneous recording of neural responses in the inferior colliculus [30], [34]. This is a prototype of a cochlear nucleus auditory prosthesis to restore hearing to deaf persons who cannon benefit from a cochlear implant, due to a loss of the auditory nerves. Excluding one electrically open site, the 15 usable stimulation sites had an average geometric surface area of 2,152 ± 91 μm^2. Located on four shanks of the multisite silicon-substrate array, the gold electrode sites were electroplated with iridium oxide to increase the stimulus charge transfer capacity to a 17 ± 3 mC/cm^2 in phosphate buffered saline (measured by cyclic voltammetry with a scan rate of 50 mV/s and between −0.6 V to +0.8 V vs. Ag/AgCl). The single-channel bipolar macroelectrode for recording of ENRs (a pair of stainless steel wires, 100 μm in diameter, insulated with Parylene C) was implanted in the contralateral inferior colliculus. The graphic user interface has been designed to provide a choice of amplitude-modulated rectangular pulses with a phase duration of 50–200 μs, a pulse frequency of 20–250 Hz, and pulse amplitude of 10–40 μA. However, the controller hardware can accommodate a much greater stimulus charge per phase for an application that might so require (e.g., stimulation with macroelectrodes rather than microelectrodes).

The animal was outfitted with a torso vest which held the controller (Fig. 6). Using the percutaneous head connector, the controller was connected to the stimulating array in the cochlear nucleus and the recording electrode in inferior colliculus, both chronically implanted for one month. The animal did not display any signs of distress during the stimulation of any of the sites in the cochlear nucleus at amplitude of 20 μA (3 nC/phase).

The controller allows interleaved (sequential) or simultaneous stimulation with all 16 electrodes, or a subset of these, and simultaneous recording of the SVW data from the stimulated electrode. The ENR data is recorded in the intervals between the stimulation pulses.

The overall performance of the recording and transmitting part of the controller was tested by continuous acquisition of the ENR signal. The frequency response was 17 Hz to 5.3 kHz (attenuation <= − 3 dB) and the RMS noise over this passband was 7.8 μV.

The first tested function was the measurement of the impedance of the stimulating electrode sites at 30 days after implantation. The total impedance across the electrode–tissue interface is comprised of the impedance of the surrounding tissue, usually designated as the "access impedance," and the electrode site impedance (polarization of the electrode-electrolyte interface during injection of the stimulus charge). The access impedance is primarily resistive and is measured as the initial fall (for cathodic pulses) or rise (for anodic pulses) of the SVW and represents the primarily resistive access impedance component, while the subsequent slower change in the SVW represents the polarization across the electrode–tissue interface [20], [35]. The SVW data was recorded from 15 electrodes during injection of rectangular current pulses with amplitude of 20 μA [Fig. 7(a)]. The access impedance values were calculated at 15 μs after pulse initiation, and for all electrodes they were in the range of 80–140 kΩ, which is typical of chronically-implanted iridium oxide-plated microelectrodes with a surface area of ~ 2000 μm^2.

We then acquired the ENRs from the bipolar electrode chronically implanted in the cat's inferior colliculus. The ENRs were recorded for 9 ms following each stimulus pulse pair applied in the cochlear nucleus at 10,20, and 30 μA (Fig. 8). Increasing the pulsing amplitude from 10 to 30 μA produced a corresponding increase in the ENR for all electrodes. The initial portion of the record immediately after the end of the stimulus pulse shows a lack of stimulus-related artifact and the controller's ability to record an early ENR in the inferior colliculus at less than 100 μs after the end of the stimulus pulse applied in the cochlear nucleus [Fig. 8(d)].

IV. Discussion

We designed and tested a novel bidirectional telemetry controller for implementing flexible protocols of mutichannel neural stimulation and recording. While some of the previous controllers also utilize the COTS ICs and bidirectional telemetry, our device features several unique capabilities, including the ability to simultaneously stimulate with up to 16 electrodes with easily configurable controlled-current waveforms, recording of the stimulus voltage waveforms, and the use of stimulus artifact-blanking for recording of evoked neuronal activity immediately following the end of each stimulus pulse (Table II).

A key feature of our prototype is the completely independent control of the amplitude and temporal interrelationship of the stimulus injected by each of the 16 stimulating electrode, enabling current steering that can be used for "sculpting" the spatial distribution of the stimulus [36].

The use of high-capacity rechargeable batteries in the wearable controller allowed us to utilize the Bluetooth communication for up to 8 h of continuous bidirectional data transmission. The Bluetooth transmission rate of 0.5 Mb/s was considerably greater than is possible using analog RF telemetry and features automatic error detection and correction. The last three entries in Table II represent the controllers that provide a high number of stimulating or recording channels and high data throughput, but they are limited to unidirectional telemetry and do not provide integration of recording and stimulation features. Moreover, these devices use

proprietary IC components, which make these systems considerably more expensive and less flexible.

Another unique feature of our wireless device is the ability to record the stimulus voltage waveforms, allowing regular and frequent monitoring of the stimulating electrode's impedance. The computer-based controller can be programmed to automatically turn off the stimulation at an individual site if a sudden increase or decrease in the site's impedance is detected.

The addition of the stimulus artifact-blanking circuitry into the ENR subsystem significantly improved the ability to record the neuronal activity immediately following the stimulus pulse. Other devices lacking the stimulus blanking, such as the Neurochip, employ rapid-recovery amplifiers that remain saturated for 100–150 μs following each stimulation pulse [41]. In contrast, the blanking circuitry on our device protects the amplifiers from saturation by stimulus artifacts and makes them available for recording within 15 μs after the end of the stimulus pulse. Monitoring of early neuronal responses is especially important in evaluating neural structures in which there is a short latency of action potential propagation between the sites of stimulation and recording. In the feline brainstem, for example, the distance between the inferior colliculus and the cochlear nucleus is a few mm and the onset of the evoked response was seen at less than 0.5 ms after the end of the stimulus pulse.

In summary, we have demonstrated a bidirectional telemetry controller with a flexible and scalable design, user-friendly computer interface, and a set of features that are should expedite *in vivo* animal testing during the development of neuroprosthetic devices.

Supplementary Material

Refer to Web version on PubMed Central for supplementary material.

Acknowledgments

Preparation of the multisite silicon probes (probe grinding and cleaning) was performed by V. Cheng. Assembly of the probes into arrays was done by N. Kuleviciute. Electroplating and laser processes were performed by Y. Smirnova. The authors would like to thank E. Smith for surgical assistance and J. E. Lemke and F. Prater for animal care. The animal studies were conducted under a protocol approved by the HMRI Animal Care and Use Committee, according to the standards set forth in the Guide for the Care and Use of Laboratory Animals. HMRI has an animal use assurance on file with the National Institutes of Health (A3606-01).

This work of D. B. McCreery was provided by the National Institutes of Health (NIH) under Grant R01-DC009643 and Grant R01-NS054121. The work of V. Pikov was supported by the NIH under Grant R01-NS057287.

References

1. Fayad JN, Otto SR, Shannon RV, et al. Neural interface for hearing restoration: Cochlear and brain stem implants. Proc IEEE Jul;2008 96(no. 7):1085–1095.
2. Weiland JD, Humayun MS. Visual prosthesis. Proc IEEE Jul;2008 96(no. 7):1076–1084.
3. Liker MA, Won DS, Rao VY, et al. Deep brain stimulation: An evolving technology. Proc IEEE Jul; 2008 96(no. 7):1129–1141.
4. Amar AP, Levy ML, Liu CY, et al. Vagus nerve stimulation. Proc IEEE Jul;2008 96(no. 7):1142–1151.
5. Lin V, Hsiao IN. Functional neuromuscular stimulation of the respiratory muscles for patients with spinal cord injury. Proc IEEE Jul;2008 96(no. 7):1096–1107.
6. Pikov V. Clinical applications of intraspinal microstimulation. Proc IEEE Jul;2008 96(no. 7):1120–1128.
7. He J, Ma C, Herman R. Engineering neural interfaces for rehabilitation of lower limb function in spinal cord injured. Proc IEEE Jul;2008 96(no. 7):1152–1166.

8. Donoghue JP, Nurmikko A, Black M, et al. Assistive technology and robotic control using motor cortex ensemble-based neural interface systems in humans with tetraplegia. J Physiol Mar 15;2007 579(pt. 3):603–611. [PubMed: 17272345]
9. Loeb GE, Richmond FJ, Baker LL. The BION devices: Injectable interfaces with peripheral nerves and muscles. Neurosurg Focus 2006;20(no. 5):E2. [PubMed: 16711659]
10. Moxon, KA.; Morizio, J.; Chapin, JK., et al. Designing a brain-machine interface for neuroprosthetic control. In: Moxon, KA.; Chapin, JK., editors. Neural Prostheses for Restoration of Sensory and Motor Function. Boca Raton Fl: CRC Press; 2000.
11. Kimmich, HP. Biotelemetry. In: Webster, JG., editor. Encyclopedia of Medical Devices and Instrumentation Biotelemetry. New York: Wiley; 1988. p. 409-425.
12. Proakis, JG.; Salehi, M. Communication Systems Engineering. 2. Englewood Cliffs, Nj: Prentice Hall; 2001.
13. Zierhofer CM, Hochmair IJ, Hochmair ES. The advanced Combi 40+ cochlear implant. Am J Otol Nov;1997 18(no. 6):S37–S38. [PubMed: 9391589]
14. Brown CJ, Abbas PJ, Gantz BJ. Preliminary experience with neural response telemetry in the nucleus CI24M cochlear implant. Am J Otol May;1998 19(no. 3):320–327. [PubMed: 9596182]
15. Suaning GJ, Lovell NH. CMOS neurostimulation ASIC with 100 channels, scaleable output, and bidirectional radio-frequency telemetry. IEEE Trans Biomed Eng Feb;2001 48(no. 2):248–260. [PubMed: 11296881]
16. Ritchie A, Howard W. Recent developments and likely advances in lithium-ion batteries. J Power Sources 2006;162(no. 2):809–812.
17. Hao Y, Foster R. Wireless body sensor networks for health-monitoring applications. Physiol Meas Nov;2008 29(no. 11):R27–R56. [PubMed: 18843167]
18. Ye X, Wang P, Liu J, et al. A portable telemetry system for brain stimulation and neuronal activity recording in freely behaving small animals. J Neurosci Methods Sep 30;2008 174(no. 2):186–193. [PubMed: 18674564]
19. Erasala N, Yen DC. Bluetooth technology: A strategic analysis of its role in global 3G wireless communication era. Computer Standards Interfaces 2002;24(no. 3):193–206.
20. Cogan SF. Neural stimulation and recording electrodes. Annu Rev Biomed Eng 2008;10:275–309. [PubMed: 18429704]
21. Robblee LS, Lefko J, Brummer SB. Activated IR: An electrode suitable for reversible charge injection in saline solution. J Electrochem Soc 1983;130:731–733.
22. McCreery DB, Agnew WF, Yuen TG, et al. Charge density and charge per phase as cofactors in neural injury induced by electrical stimulation. IEEE Trans Biomed Eng Oct;1990 37(no. 10):996–1001. [PubMed: 2249872]
23. McCreery DB, Bullara LA, Agnew WF. Neuronal activity evoked by chronically implanted intracortical microelectrodes. Exp Neurol 1986;92(no. 1):147–161. [PubMed: 3956646]
24. McCreery DB, Yuen TG, Agnew WF, et al. Stimulation with chronically implanted microelectrodes in the cochlear nucleus of the cat: Histologic and physiologic effects. Hear Res 1992;62(no. 1):42–56. [PubMed: 1429250]
25. McCreery DB, Yuen TG, Agnew WF, et al. Stimulus parameters affecting tissue injury during microstimulation in the cochlear nucleus of the cat. Hear Res 1994;77(no. 1–2):105–115. [PubMed: 7928722]
26. McCreery DB, Yuen TG, Agnew WF, et al. A characterization of the effects on neuronal excitability due to prolonged microstimulation with chronically implanted microelectrodes. IEEE Trans Biomed Eng Oct;1997 44(no. 10):931–939. [PubMed: 9311162]
27. McCreery DB, Yuen TG, Bullara LA. Chronic microstimulation in the feline ventral cochlear nucleus: Physiologic and histologic effects. Hear Res 2000;149(no. 1–2):223–238. [PubMed: 11033261]
28. McCreery D, Pikov V, Lossinsky A, et al. Arrays for chronic functional microstimulation of the lumbosacral spinal cord. IEEE Trans Neural Syst Rehabil Eng Jun;2004 12(no. 2):195–207. [PubMed: 15218934]
29. McCreery DB, Agnew WF, Bullara LA. The effects of prolonged intracortical microstimulation on the excitability of pyramidal tract neurons in the cat. Ann Biomed Eng 2002;30(no. 1):107–119. [PubMed: 11874134]

30. McCreery D, Lossinsky A, Pikov V. Performance of multisite silicon microprobes implanted chronically, in the ventral cochlear nucleus of the cat. IEEE Trans Biomed Eng Jun;2007 54(no. 6): 1042–1052. [PubMed: 17554823]

31. McCreery D, Lossinsky A, Pikov V, et al. A microelectrode array for chronic deep brain stimulation and recording. IEEE Trans Biomed Eng Apr;2006 53(no. 4):726–737. [PubMed: 16602580]

32. Pikov V, Bullara L, McCreery DB. Intraspinal stimulation for bladder voiding in cats before and after chronic spinal cord injury. J Neural Eng 2007;4(no. 4):356–368. [PubMed: 18057503]

33. Han, M.; Bullara, LA.; McCreery, DB. Proc BMES Meeting. Los Angeles, CA: 2007. Development of a robust chronic neural probe; p. P2-146.

34. McCreery DB. Cochlear nucleus auditory prostheses. Hear Res Aug;2008 242(no. 1–2):64–73. [PubMed: 18207678]

35. Tykocinski M, Cohen LT, Cowan RS. Measurement and analysis of access resistance and polarization impedance in cochlear implant recipients. Otol Neurotol Sep;2005 26(no. 5):948–956. [PubMed: 16151342]

36. Butson CR, McIntyre CC. Current steering to control the volume of tissue activated during deep brain stimulation. Brain Stimulat Jan;2008 1(no. 1):7–15. [PubMed: 19142235]

37. Jackson A, Moritz CT, Mavoori J, et al. The neurochip BCI: Towards a neural prosthesis for upper limb function. IEEE Trans Neural Syst Rehabil Eng Jun;2006 14(no. 2):187–190. [PubMed: 16792290]

38. Farshchi S, Pesterev A, Nuyujukian PH, et al. Bi-Fi: An embedded sensor/system architecture for REMOTE biological monitoring. IEEE Trans Inf Technol Biomed Nov;2007 11(no. 6):611–618. [PubMed: 18046936]

39. Ghovanloo M, Najafi K. A wireless implantable multichannel microstimulating system-on-a-chip with modular architecture. IEEE Trans Neural Syst Rehabil Eng Sep;2007 15(no. 3):449–457. [PubMed: 17894278]

40. Triangle-BioSystems. Neural Stimulation [Online]. Available: www.trianglebiosystems.com/Products/NeuralStimulation.aspx

41. Mavoori J, Millard B, Longnion J, et al. A miniature implantable computer for functional electrical stimulation and recording of neuromuscular activity. 2004 IEEE Int Workshop Biomed Circ Syst 2004:S1.7.INV.13–S1.7.INV.16.

Biographies

Vishnu Sharma received the B.Eng. degree in I&C Eng. from the South Gujarat University, Surat, India, in 2002, and the M.S. in biomedical engineering from the Louisiana Tech University, Ruston, in 2007. His M.S. research involved developing finite element model to study the effects of concentric ring electrode electrical stimulation on the rat skin.

He worked as Biomedical Engineer at the Huntington Medical Research Institutes, Pasadena, CA, designing low power custom analog and digital circuits for stimulation and recording. His

research interests include neural prostheses, functional electrical stimulation, and obstructive sleep apnea.

Douglas B. McCreery received the B.S. in electrical engineering and the Ph.D. degree in biomedical engineering from the University of Connecticut, in 1966 in 1975, respectively. He completed his postdoctoral training in neurosurgery and neurophysiology at the University of Minnesota.

He joined the Huntington Medical Research Institutes, Pasadena, CA, in 1979 and became the Director of the Neural Engineering Program in 2001. His research interests include the development of sensory and motor neuroprostheses and devices for neuromodulation of the central nervous system, and the physiologic and histologic effects of electrical stimulation of the central and peripheral nervous systems.

Martin Han (M'04) received the B.S. degree in electrical engineering from the University of Hawaii at Manoa, Honolulu, HI, in 1996, and the M.S. degree in electrical engineering and the Ph.D. degree in biomedical engineering from the University of Southern California, Los Angeles, in 2000 and 2003, respectively. His Ph.D. dissertation focused on the development of planar microelectrode arrays for recording and stimulation in hippocampal tissue slices in the development of cognitive prosthesis.

Since 2003, he is a Staff Scientist in the Neural Engineering Program at Huntington Medical Research Institutes, Pasadena, CA. His research interests include development of silicon- and biodegradable polymer-based chronically-implantable microelectrode arrays using bio-MEMS technology for treatment of neurological disorders such as profound hearing loss, Parkinson's disease, and spinal cord injury.

Dr. Han is a member of the Eta Kappa Nu, Society for Neuroscience, and American Association for the Advancement of Science.

Victor Pikov received the BA. degree (*cum laude*) in biopsychology and computer sciences at Vassar College, Poughkeepsie, NY, and the Ph.D. degree in cell biology and neuroscience from Georgetown University, Washington, DC. He completed the postdoctoral training in molecular biology at the California Institute of Technology, Pasadena, in 2002.

He joined the Neural Engineering Laboratory at Huntington Medical Research Institutes (HMRI), Pasadena, CA. At HMRI, he works as a Neurophysiologist and Neural Engineer and since 2005 also as a Director of the Summer Undergraduate Research Program. His research interests include the evaluation of efficacy and safety of electrical and electromagnetic stimulation in the central nervous system, with an emphasis on the spinal control of bladder

function, brainstem involvement in tinnitus, and corticospinal excitability in stroke. In addition to his research duties, he is a founder and co-chair of the International Conferences on Neuroprosthetic Devices in Taiwan and China and an Associate Editor for the journal *Frontiers in Neuroprosthetics*.

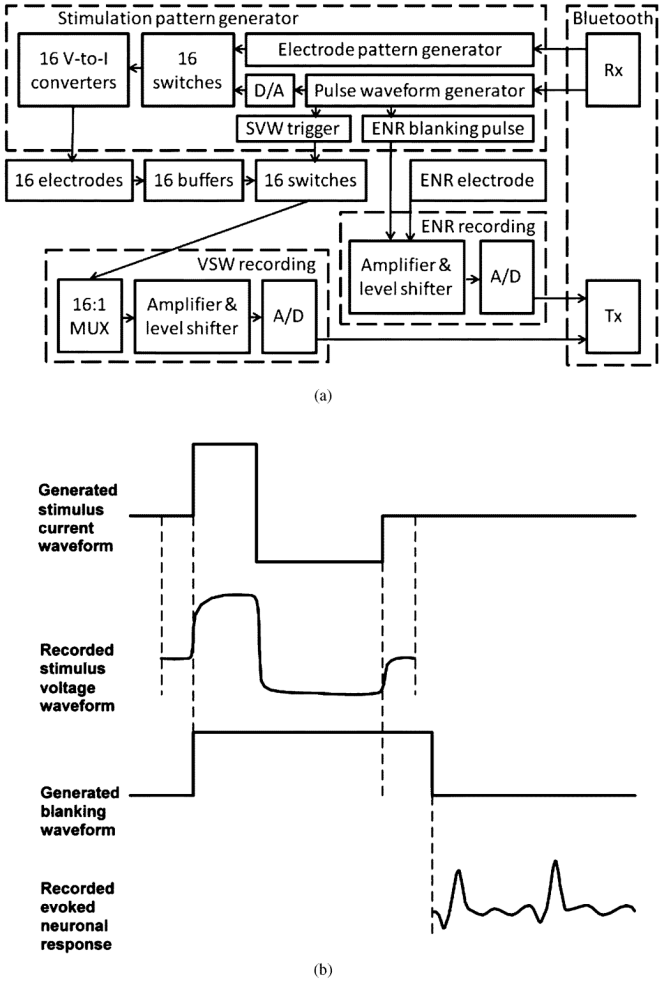

Fig. 1.

(a) Functional block diagram of the wearable controller. Abbreviations: A/D and D/A—analog-to-digital and digital-to-analog converters, MUX—multiplexer, Rx—reception of data, Tx—transmission of data, V-to-I—voltage-to-current. (b) Temporal sequence of the generated current stimulus waveform and blanking waveform relative to the recorded stimulus voltage waveform and evoked potential response.

Fig. 2.
The wearable controller: (a), (b) three interconnected printed circuit boards in the expanded and collapsed states, (c) the controller in plastic enclosure and with a cable for connection to the implanted 16-electrode array.

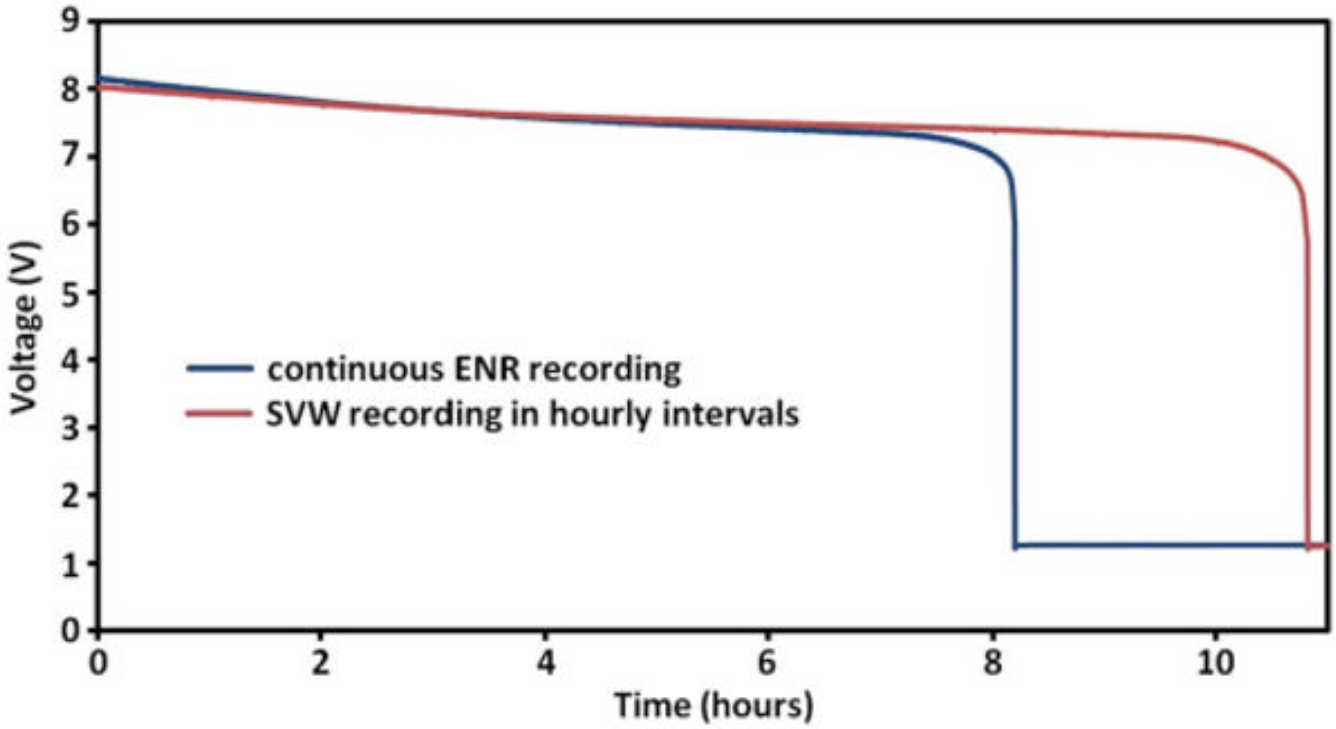

Fig. 3.
Tests of battery life of wearable controller in two operating modes: continuous ENR recording and SVW recording in hourly intervals.

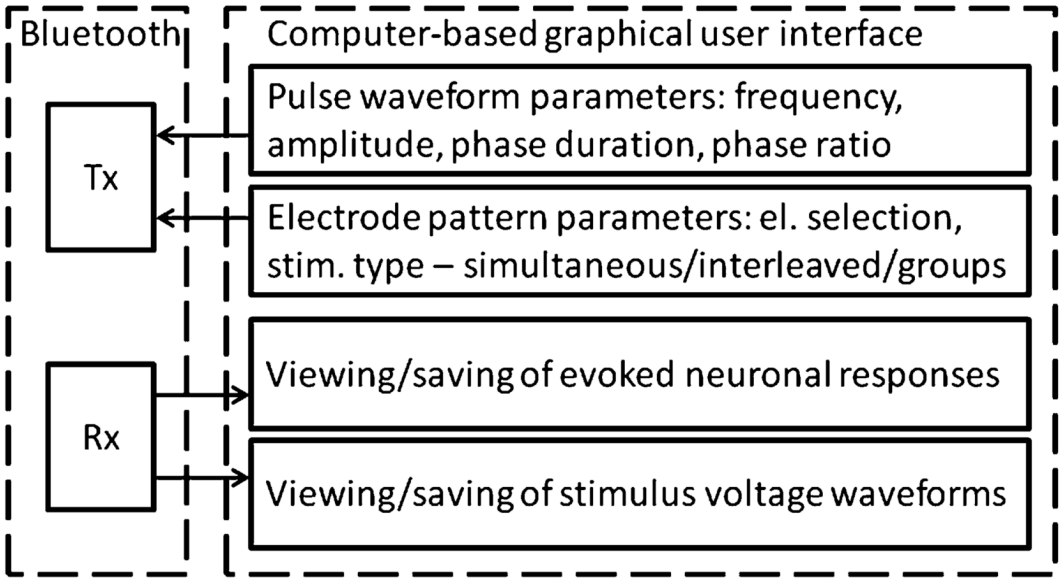

Fig. 4.
Functional block diagram of the computer-based controller. Abbreviations: Rx—reception of data, Tx—transmission of data.

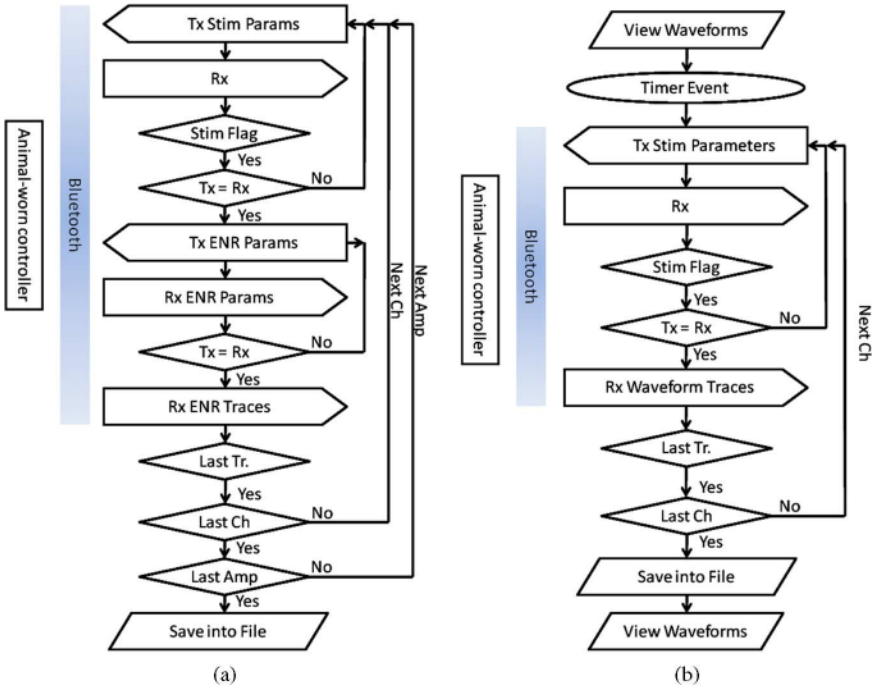

Fig. 5.

Flow charts of two data acquisition events. (a) User-initiated acquisition of the evoked neuronal responses (ENR) during stimulation with averaging of a specified number of recordings (traces) per stimulation amplitude. (b) Quasi real-time viewing and periodic saving of the stimulus voltage waveforms. Abbreviations: Rx—reception of data, Tx—transmission of data. Flowchart shapes: rectangle with the left or right arrow—Tx or Rx event, parallelogram—data output to a computer monitor (for viewing) or hard disk (for saving), oval—delay until counter/timer event, diamond—decision event with Yes-No options.

Fig. 6.
Animal wearing the torso vest with the attached controller for bidirectional telemetry.

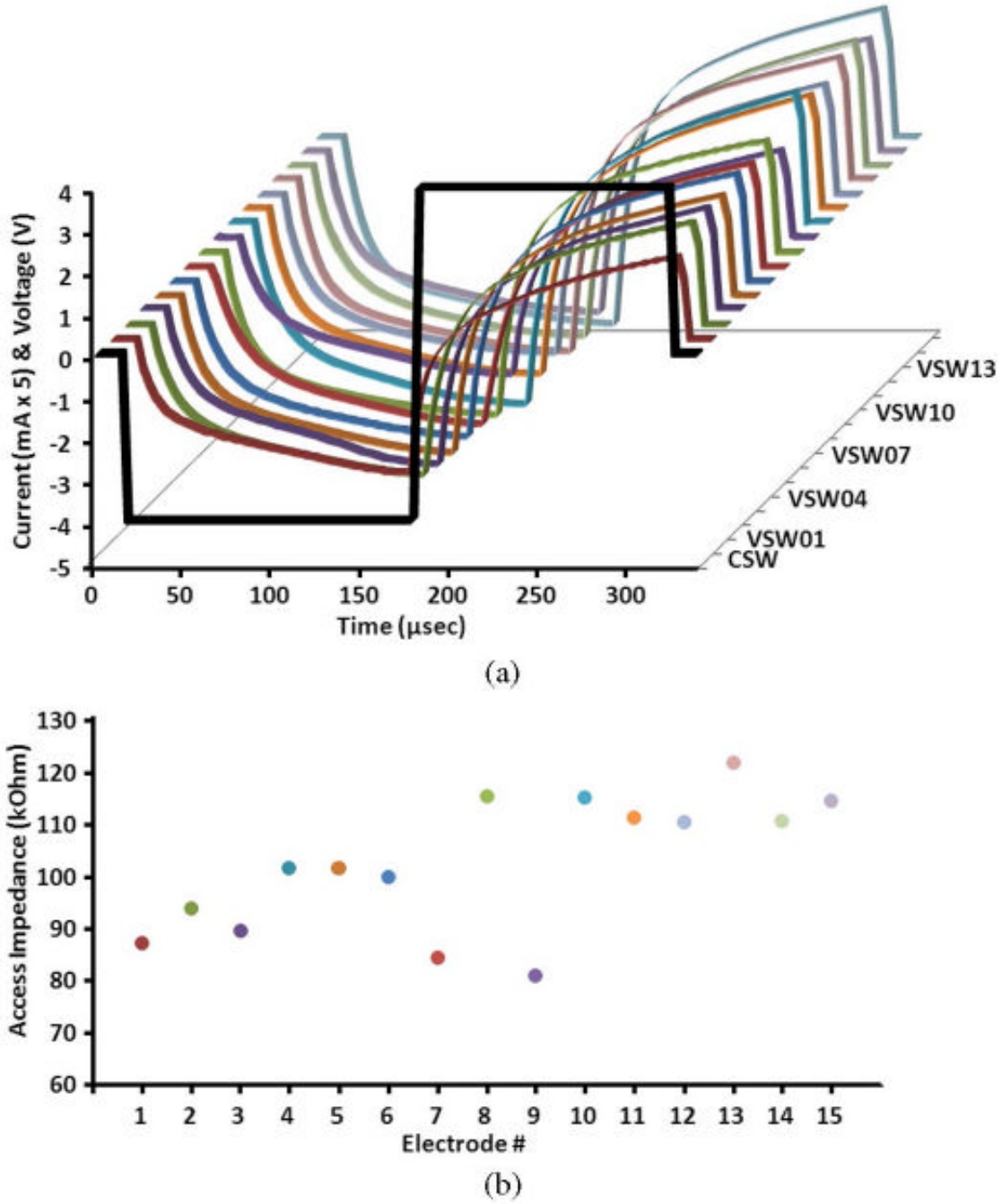

Fig. 7.

(a) Stimulus voltage waveforms (SVWs) recorded from 15 electrodes in the feline cochlear nucleus during pulsing of these electrodes with the biphasic rectangular current stimulus waveform (CSW). (b) Access impedances of pulsed electrodes, calculated from the SVWs at 15 μs after pulse initiation.

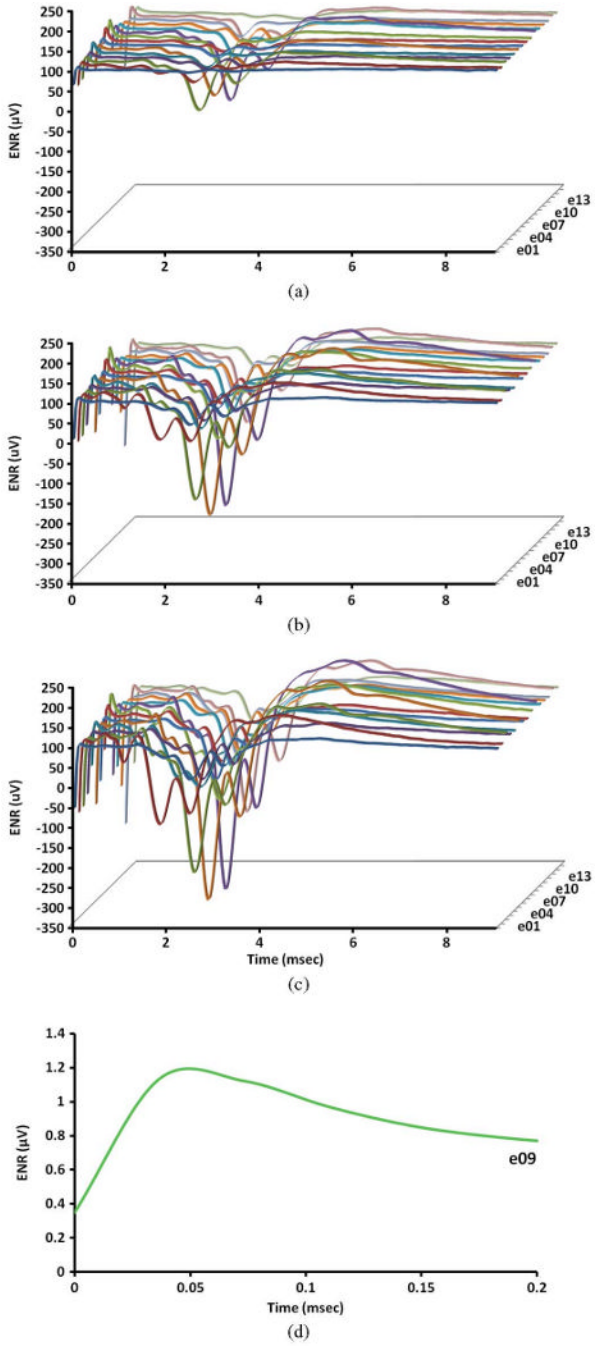

Fig. 8.

Evoked neuronal responses (ENRs) in the cat's inferior colliculus produced by stimulating with each of the 15 microelectrodes in the contralateral cochlear nucleus. Panels A, B, and C represent ENRs induced using a stimulus amplitude of 10, 20, and 30 μA. Panel D is a zoomed-in view of the ENR at electrode 9 induced by 30 μA.

Table I

Functionality of the integrated chip (IC) components in the wearable controller (In the order of decreasing power consumption).

Component	IC model, company	Key IC features	Current, mA	Power cons., mW
Bluetooth communication	F2M03GLA, Free2move	Bluetooth V.2.0+EDR, UART	44/22*	145/73*
Rx from Bluetooth, PWG & EPG	PIC18F4620, Microchip Tech.	3K RAM, 1K EEPROM, UART, SPI	21/10*	105/50*
Tx to Bluetooth	PIC18F2620, Microchip Tech.	3K RAM, 1K EEPROM, UART, SPI	21/10*	105/50*
16-ch. V-to-I converter (Howland pump)	TLV2741 × 8, Texas Instruments	R-R output, high GBW & SR	3.2 per ch.	19 per ch.
D/A converter	TLV5626, Texas Instruments	8 bit, 0.28/sec, SPI	3.7	18.5
Amplifier & voltage shifter	TLV271 × 2, Texas Instruments	R-R output, high GBW & SR	1.1	17.6
A/D converter	ADS7886, Texas Instruments	12 bit, 1 Ms/sec, SPI	1.5	7.5
16-ch. analog switch for electrode grounding	PS393 × 4, Pericom	Low leakage current (<2 pA)	0.004	0.064
16-ch. analog switch for stimulation selection	PS393 x 4, Pericom	Low leakage current (<2 pA)	0.004	0.064
16:1 analog MUX for recording selection	MAX396, Maxim	Low leakage current (30 pA)	0.001	0.016
Total			96/52*	418/236*

In the Current and Power consumption columns, the second value, marked by asterisk (*), indicates an idle state. Abbreviations: A/D—analog-to-digital, consump.—consumption, D/A—digital-to-analog, EDR—Enhanced Data Rate, GBW—gain bandwidth product, Ms—megasamples; PWG & EPG—pulse waveform generator and electrode pattern generator, SPI—serial peripheral interface bus, SR—slew rate, R-R—rail-to-rail, Tx—transmission of data, UART—universal asynchronous receiver/transmitter bus, V-to-I—voltage-to-current

Table II

Comparison of Wireless Controllers Used for Transmission of Neural Data

Controller	Max # of rec. chs	Max # of stim. chs	SAB	Telemetry	Sustained data rate	COTS ICs	Ref.
HMRI	16 seq.	16 sim.	yes	bidir. Bluetooth	500 kbps	yes	This article
Zhe jiang U.	2 sim.	4 seq.	no	bidir. Bluetooth	461 kbps	yes	[18]
Neurochip	12 seq.	12 seq.	no	bidir. IR	94 kbps	yes	[37]
Bi-Fi	8 seq.	none	N/A	bidir. 802.15.4	96 kbps	yes	[38]
Interestim-2B	none	32 seq./8 sim.	N/A	unidir. phase-coherent FSK	2.5Mbps	no	[39]
TBSI W63	63 sim.	none	N/A	unidir. AWFM	3.3 Msps	no	[40]
Neuralynx Digital Falcon	32 sim.	none	N/A	unidir. UWB	24 Mbps	no	

Abbreviations: AWFM mod.—analog wideband frequency modulation, bidir.—bidirectional, bps—bit per second, COTS ICs—commercial off-the-shelf integrated circuits, FSK—frequency shift keyed, IR—infrared, N/A—not applicable, SAB—stimulus artifact-blanking, seq.—sequential use, sim.—simultaneous use, sps—samples per second, unidir.—unidirectional, UWB—ultra-wideband